

HIV-1 Tat Induces Unfolded Protein Response and Endoplasmic Reticulum Stress in Astrocytes and Causes Neurotoxicity through Glial Fibrillary Acidic Protein (GFAP) Activation and Aggregation^{*[5]}

Received for publication, April 9, 2016, and in revised form, August 31, 2016. Published, JBC Papers in Press, September 8, 2016, DOI 10.1074/jbc.M116.731828

Yan Fan and  Johnny J. He¹

From the Department of Cell Biology and Immunology, Graduate School of Biomedical Sciences, University of North Texas Health Science Center, Fort Worth, Texas 76107

HIV-1 Tat is a major culprit for HIV/neuroAIDS. One of the consistent hallmarks of HIV/neuroAIDS is reactive astrocytes or astrogliosis, characterized by increased cytoplasmic accumulation of the intermediate filament glial fibrillary acidic protein (GFAP). We have shown that Tat induces GFAP expression in astrocytes and that GFAP activation is indispensable for astrocyte-mediated Tat neurotoxicity. However, the underlying molecular mechanisms are not known. In this study, we showed that Tat expression or GFAP expression led to formation of GFAP aggregates and induction of unfolded protein response (UPR) and endoplasmic reticulum (ER) stress in astrocytes. In addition, we demonstrated that GFAP up-regulation and aggregation in astrocytes were necessary but also sufficient for UPR/ER stress induction in Tat-expressing astrocytes and for astrocyte-mediated Tat neurotoxicity. Importantly, we demonstrated that inhibition of Tat- or GFAP-induced UPR/ER stress by the chemical chaperone 4-phenylbutyrate significantly alleviated astrocyte-mediated Tat neurotoxicity *in vitro* and in the brain of Tat-expressing mice. Taken together, these results show that HIV-1 Tat expression leads to UPR/ER stress in astrocytes, which in turn contributes to astrocyte-mediated Tat neurotoxicity, and raise the possibility of developing HIV/neuroAIDS therapeutics targeted at UPR/ER stress.

HIV-1 infection of the CNS leads to neurologic disorders, such as the rare HIV-associated dementia, and the more prevalent mild form as minor cognitive motor disorder, which is collectively called HIV/neuroAIDS (1–3). Although the introduction of combination antiretroviral therapy has increased the lifespan of HIV-infected individuals, it has failed to prevent HIV/neuroAIDS or to reverse the disease in most of the cases (4). Because the underlying cellular and molecular mechanisms remain poorly understood, there are no effective therapies to

reduce, prevent, or reverse HIV-mediated cognitive, learning, and memory dysfunction at the present time.

The primary cell targets of HIV-1 in the CNS are macrophages/microglia, whereas neurons are indirectly affected through mechanisms such as immune dysregulation, release of toxic soluble viral protein from HIV-infected cells, and the disruption of brain homeostasis (2, 5–8). HIV-1 trans-activator of transcription (Tat) is considered to be a major culprit for HIV-associated neurocognitive disorder (7–10). Tat is secreted from HIV-infected cells in the CNS, such as microglia/macrophages and astrocytes, and then taken up by other uninfected CNS cells (11–13). Evidence has accumulated to suggest that Tat adversely affects neurons in both direct and indirect manners; direct Tat exposure alters neuronal integrity, disrupts homeostasis, and promotes oxidative stress (14–16). Tat could also affect neuronal survival indirectly by recruiting immune cells into the CNS or by altering neuronal gene expression profiles and intracellular signaling cascades (13, 17–23). Recent studies have shown that astrocytes play important roles in mediating Tat neurotoxicity and HIV/neuroAIDS (24–26).

HIV-1 infection of astrocytes has been detected both *in vivo* and *in vitro* (25, 27). It has been characterized as a consistent and restricted form, in which HIV-1 early proteins such as Nef and Tat are abundantly expressed, but not the structural proteins. Production of new HIV-1 virions in those cells is severely restricted through viral entry, transcription, and post-translational modification and assembly (24, 28–31). As a compartment of the blood-brain barrier, astrocytes facilitate the invasion of HIV-1 into the CNS. HIV infection of astrocytes promotes secretion of cytokines/chemokines, which potentiates the infiltration of infected immune cells and spread of HIV and its toxic proteins among those cells in the CNS (26, 32–39). Importantly, the activation of astrocytes, also known as astrogliosis, which is characterized by increased accumulation of the intermediate filament GFAP,² has been a consistent hallmark of HIV/neuroAIDS. GFAP, an astrocyte-specific cell marker, is a critical regulator of Tat neurotoxicity (40–45),

^{*} This work was supported by NINDS, National Institutes of Health Grants R01NS065785, R01094108, and R01MH092673 (to J. J. H.). The authors declare that they have no conflicts of interest with the contents of this article. The content is solely the responsibility of the authors and does not necessarily represent the official views of the National Institutes of Health.

^[5] This article contains supplemental Figs. S1–S3.

¹ To whom correspondence should be addressed: Dept. of Cell Biology and Immunology, Graduate School of Biomedical Sciences, University of North Texas Health Science Center, 3500 Camp Bowie Blvd., Fort Worth, TX 76107. Tel.: 817-735-2642; Fax: 817-735-0181; E-mail: johnny.he@unthsc.edu.

² The abbreviations used are: GFAP, glial fibrillary acidic protein; UPR, unfolded protein response; ER, endoplasmic reticulum; RIPA, radioimmune precipitation assay; PERK, PKR-like ER kinase; BiP, binding immunoglobulin protein; OASIS, old astrocyte specifically induced substance; 4-PBA, 4-phenylbutyrate; Dox, doxycycline; MTT, 3-(4,5-dimethylthiazol-2-yl)-2,5-diphenyl tetrazolium bromide.

Tat Activation of UPR/ER Stress in Astrocytes

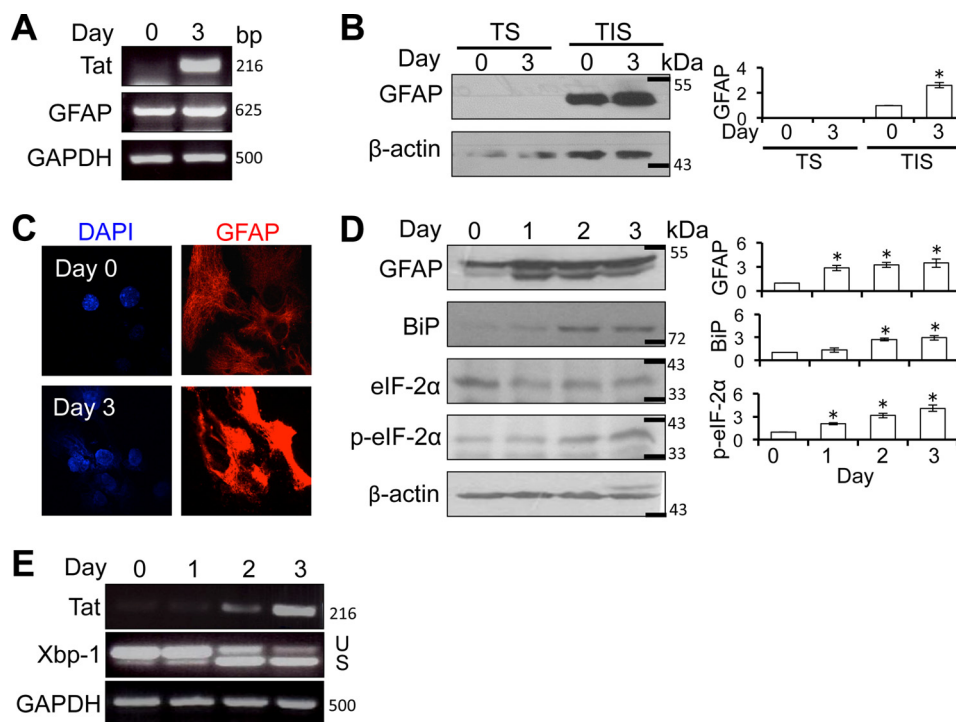


FIGURE 1. Tat expression increased eIF-2 α phosphorylation and Xbp-1 alternate splicing in astrocytes. *A*, iTat primary astrocytes were cultured in the presence of 5 μ g/ml Dox for 0 and 3 days. Total RNA was isolated for RT-PCR using Tat- and GFAP-specific primers. GAPDH was included as an internal control. *B*, cell lysates of the same cells were separated into Triton X-100-soluble (TS) and insoluble (TIS) fractions and analyzed for GFAP expression by Western blotting. β -Actin was included as an equal loading control. *C*, the same cells were immunostained for GFAP expression, followed by microscopic imaging. The cells were counterstained with 100 ng/ml DAPI for nuclei. *D* and *E*, iTat primary astrocytes were cultured in the presence of 5 μ g/ml Dox for 0, 1, 2, and 3 days. Cells were analyzed for total eIF-2 α , phosphorylated eIF-2 α (p-eIF-2 α), or GFAP expression by Western blotting (*D*). β -Actin was included as an equal loading control. Total RNA was also isolated from the cells for RT-PCR using Xbp1- or Tat-specific primers (*E*). -Fold changes in protein expression over day 0 were the mean \pm S.D. (error bars) of three independent repeats and are shown to the right of the respective Western blots. GAPDH was included as an internal control. *U* and *S*, unspliced and spliced RNA-derived PCR DNA, respectively. *, $p < 0.05$.

defining what is known as astrocyte-mediated Tat neurotoxicity. However, the underlying molecular mechanisms are largely unknown.

In the study, we aimed to determine the molecular mechanisms of astrocyte-mediated Tat neurotoxicity. Using a combined molecular, cellular, biochemical, and genetic approach, we demonstrated that GFAP up-regulation by Tat induced UPR/ER stress response in astrocytes and, as a result, led to astrocyte-mediated Tat neurotoxicity. These findings uncover a novel mechanism through which Tat interacts with GFAP/astrocytes and contributes to HIV/neuroAIDS and illustrate the importance of maintaining appropriate GFAP expression in astrocytes in response to various neuronal insults or injury.

Results

Tat Expression Led to Increased GFAP Expression and Aggregation and Activation of Unfolded Protein Response (UPR)/Endoplasmic Reticulum (ER) Stress—Our previous studies have shown that Tat expression alone is sufficient to activate GFAP expression and induce astrocytosis and astrocyte-mediated neurotoxicity (40, 46–48). Using primary astrocytes obtained from the doxycycline-inducible astrocyte-specific HIV-1 Tat transgenic mice (iTat), we confirmed that Tat expression resulted in GFAP up-regulation at the mRNA level (Fig. 1A). GFAP expression in astrocytes (day 0) exhibited a cytoskeletal array of fine filaments throughout the cytoplasm (Fig. 1C, top), whereas astrocytes that were cultured in the presence of Dox

(day 3) showed strong GFAP aggregates/inclusions around the nuclei, often with disruption of the normal filament architecture in the immediate vicinity of the inclusion (Fig. 1C, bottom). To further determine intracellular GFAP localization and aggregation, we prepared cell lysates from astrocytes at day 0 and 3 of Dox treatments first using the regular RIPA buffer and then further extracted the pellets with RIPA buffer containing 1% Triton X-100. We then analyzed GFAP in the lysates from regular RIPA buffer (soluble) and from the RIPA buffer containing 1% Triton X-100 (insoluble) using Western blotting. As expected, GFAP in both astrocytes was detected almost exclusively in the insoluble fraction (Fig. 1B). These results indicate that Tat-activated GFAP expression leads to the formation of GFAP aggregates and alteration of the intermediate filament network in astrocytes.

Cells that cannot efficiently eliminate protein aggregates often induce UPR and ER stress (49). Increased protein expression/aggregation and UPR/ER stress have been associated with several neurodegenerative diseases, such as Alzheimer, Huntington, Parkinson, and Alexander (50–53). Thus, we next determined whether Tat-induced GFAP expression would induce UPR/ER stress in astrocytes. iTat primary astrocytes were induced to express Tat and analyzed by Western blotting for binding immunoglobulin protein (BiP), an immediate ER stress marker, and phosphorylation of eIF-2 α , a ER stress marker activated through the PKR-like ER kinase (PERK)-me-

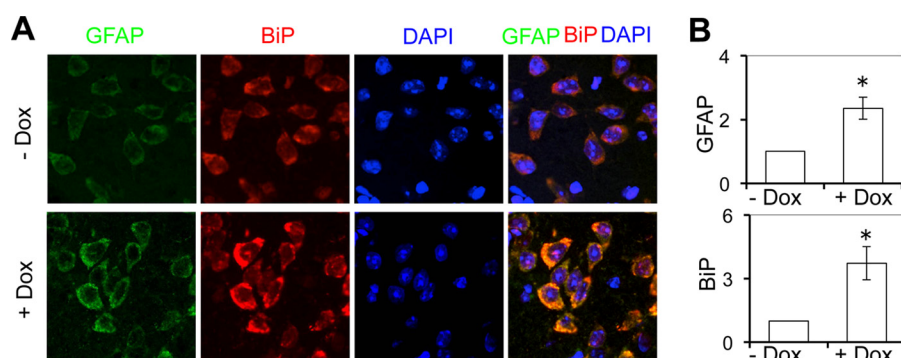


FIGURE 2. Tat expression increased BiP expression in the mouse brain. Mice (3 mice/strain) were injected i.p. with Dox (80 mg/kg/day, + Dox) or pH-matched PBS (pH 2.2, -Dox) for 7 days. The brains were collected and sectioned, and comparable cortical sections were stained with anti-GFAP or anti-BiP antibody, followed by secondary antibody goat anti-rabbit Alexa Fluor 488 or goat anti-mouse Alexa Fluor 555. The sections were then counterstained with 100 ng/ml DAPI for nuclei. The comparable cortical regions of the brains were imaged. A total of three brain sections from three Dox-treated and three PBS-treated mice were stained. The images were representative of all of the stained cortical sections in each strain (A). -Fold changes in protein expression over the control (-Dox) were the mean \pm S.D. (error bars) of multiple cortical sections from each strain and are shown beside the respective images of each group (B). *, $p < 0.05$.

diated UPR pathway (54). Increased BiP and eIF-2 α phosphorylation was noted in astrocytes in which Tat was induced and GFAP was up-regulated (Fig. 1D). Meanwhile, increased alternate splicing of Xbp-1, another ER stress marker activated through the inositol-requiring enzyme 1 (IRE1)-mediated UPR pathway (55), determined by RT-PCR, was also noted in those astrocytes (Fig. 1E). These results indicate that Tat expression led to activation of UPR/ER stress in astrocytes.

Activation of UPR/ER Stress in the Brain of Tat-expressing Mice—ER stress has been detected in the brain of HIV-infected subjects (56, 57). However, the roles of Tat in induction of ER stress in the brain of HIV-infected subjects are not known. We then took advantage of the iTat mice (58) and determined the relationship between Tat expression and ER stress in the brain. As shown previously (46–48), increased GFAP expression was detected in the brain of Dox-treated iTat mice but not in the brain of PBS-treated iTat mice (Fig. 2, A and B). In parallel, increased expression of ER stress transducer chaperone BiP (57) was noted in the brain of Dox-treated iTat mice but not in the brain of PBS-treated iTat mice. In addition, increased BiP and GFAP expression were mostly detected in the very same astrocytes. Similarly, increased BiP staining was detected in the brain of HIV-associated dementia (HAD) patients (supplemental Fig. S1). These *in vivo* results confirmed that Tat expression induced ER stress and suggest that Tat may contribute to UPR/ER stress in the brain of HIV-infected subjects.

Activation of UPR/ER Stress by GFAP Expression in Astrocytes—Next, we determined the relationship between Tat-induced GFAP expression and Tat-induced ER stress activation. To this end, we transfected primary mouse astrocytes with plasmids expressing Tat, human GFAP, or a human GFAP mutant R239H (239H) that is a common mutation associated with Alexander disease through formation of GFAP aggregates (50, 59). Western blotting was performed to determine the ER stress status in those cells using ER stress markers BiP and other markers for UPR pathways, such as PERK (phosphorylated eIF-2 α) and activating transcription factor 6 (ATF6) (54). Consistent with previous findings, Tat expression led to increased expression of BiP, phosphorylated eIF-2 α , and ATF6 when compared with the control (Fig. 3A). Both GFAP and R239H

expression also led to increased expression of BiP, phosphorylated eIF-2 α , and ATF6. In addition, those cells were analyzed by Western blotting for an astrocyte-specific ER stress marker, old astrocyte specifically induced substance (OASIS) (60). Expression of Tat, GFAP, and R239H all led to increased OASIS expression (Fig. 3, A and D) and Xbp-1 alternate splicing (Fig. 3B). Similar effects of Tat, GFAP, and R239H expression on BiP, phosphorylated eIF-2 α , ATF6, and OASIS were obtained using human primary fetal astrocytes (Fig. 3, C and D). Meanwhile, increased levels of GFAP, BiP, ATF6, and OASIS mRNA were detected in Tat-transfected mouse primary astrocytes compared with the C3-transfected cells (Fig. 3E). These results further confirmed that Tat expression induced ER stress in astrocytes and showed that GFAP expression alone was sufficient to activate UPR/ER stress in astrocytes.

Requirement of GFAP Expression for Tat-induced UPR/ER Stress in Astrocytes—Loss of neuronal integrity has been detected in the brain of HIV-infected individuals (61, 62) and HIV-associated dementia (HAD) patients (supplemental Fig. S2). GFAP activation has been, at least in part, attributed to Tat neurotoxicity *in vivo* (46, 47). Consistent with these findings, we found that ectopic GFAP expression or Tat expression in astrocytes caused neurotoxicity (supplemental Fig. S3, A and B). In addition, using iTat/GFAP-null (iTat/GFAP $^{-}$) mice, we demonstrated that GFAP knock-out significantly decreased astrocyte-mediated Tat neurotoxicity *in vitro* (Fig. 4A) and, accordingly, decreased BiP activation (Fig. 4, B and D) and formation of shortened dendrites (Fig. 4, C and E) in the cortex of iTat mice. To determine whether GFAP activation was directly involved in Tat-induced ER stress in astrocytes, we took advantage of the iTat/GFAP $^{-}$ mice and compared expression of ER stress markers in Tat-expressing astrocytes with GFAP (iTat) and without GFAP (iTat/GFAP $^{-}$). As demonstrated above, increased expression of BiP, phosphorylated eIF-2 α , ATF6, and OASIS was detected in Tat-expressing astrocytes (iTat) over Tat induction (Fig. 5A). In contrast, expression of BiP, phosphorylated eIF-2 α , ATF6, and OASIS showed no apparent changes in iTat/GFAP $^{-}$ astrocytes. Similarly, Xbp-1 alternate splicing showed increases in iTat astrocytes but no changes in iTat/GFAP $^{-}$ astrocytes (Fig. 5B). In addition, increased levels of

Tat Activation of UPR/ER Stress in Astrocytes

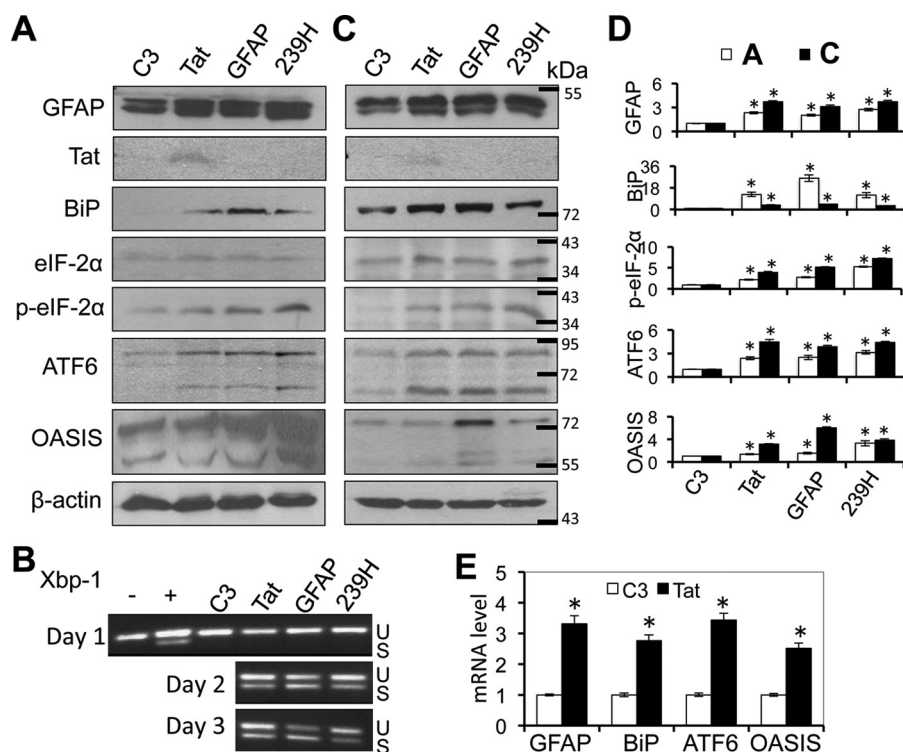


FIGURE 3. Ectopic GFAP expression activated ER stress in astrocytes. Mouse primary astrocytes (A and B) or human primary fetal astrocytes (C) were transfected with cDNA3 (C3), Tat-Myc, GFAP, or GFAP mutant 239H expression plasmids. The cells were analyzed for GFAP, Tat (c-Myc), BiP, total eIF-2 α , phospho-eIF-2 α (p-eIF-2 α), ATF6, or OASIS expression by Western blotting at 3 days post-transfection (A and C), or the mouse astrocytes were analyzed at 1, 2, or 3 days post-transfection for Xbp-1 alternate splicing by RT-PCR (B). Treatment of mouse astrocytes with thapsigargin (500 nM) was included as a positive control (+) and PBS was included as a negative control (–) for Xbp-1 alternate splicing. U and S, unspliced and spliced RNA-derived PCR DNA, respectively. D, -fold changes in protein expression over the control (C3) were the mean \pm S.D. (error bars) of three independent repeats. Open bars, data from A; closed bars, data from C. E, total RNA was isolated from C3- and Tat-transfected mouse primary astrocytes at day 3 and analyzed for GFAP, BiP, ATF6, and OASIS mRNA expression using quantitative RT-PCR. β -Actin was included as an internal control. -Fold changes in mRNA expression over the control (C3) were the mean \pm S.D. of three independent repeats. *, $p < 0.05$.

GFAP, BiP, ATF6, and OASIS mRNA were detected in iTat astrocytes but not in iTat/GFAP– astrocytes at day 3 compared with those at day 0 (Fig. 5C). Taken together, these results show that GFAP expression was required for ER stress induction in Tat-expressing astrocytes and suggest a possible link among Tat-induced GFAP activation, ER stress in astrocytes, and astrocyte-mediated Tat neurotoxicity.

Involvement of ER Stress in Astrocyte-mediated Tat Neurotoxicity—To determine the relationship among Tat expression, GFAP expression, ER stress in astrocytes, and astrocyte-mediated Tat neurotoxicity, we first transfected U373.MG with cDNA3, Tat, or GFAP expression plasmid and treated the cells with or without 5 mM 4-phenylbutyrate (4-PBA), a chemical chaperone that is commonly used to alleviate ER stress (63, 64). Compared with the cDNA3 control, both Tat and GFAP expression led to increased BiP expression and Xbp-1 alternate splicing, which was considerably decreased in cells treated with 4-PBA (Fig. 6A). In parallel, both Tat and GFAP expression led to neurotoxicity, which was also considerably inhibited with 4-PBA treatment (Fig. 6B). Next, we used iTat astrocytes and first induced them to express Tat expression with Dox and then treated them with 0, 0.1, 1, 5, or 10 mM 4-PBA and determined BiP expression and Xbp-1 alternate splicing and the neurotoxicity. Compared with the control (day 0), Dox treatment led to increased BiP expression and Xbp-1 alternate splicing (Fig. 6C) and neurotoxicity (Fig. 6D). Treatment of iTat astrocytes with

Dox and then with increasing concentrations of 4-PBA led to gradual decreases in BiP expression, Xbp-1 alternate splicing, and the neurotoxicity. These results suggest that 4-PBA protective effects are mediated, at least in part, through ER stress and UPR pathways.

To further determine the significance of ER stress in astrocyte-mediated Tat neurotoxicity, we determined the effects of 4-PBA on BiP expression, GFAP expression, and neuronal integrity using the iTat mice. WT and iTat mice were given Dox, followed by 4-PBA. The mouse brains were collected, sectioned, and immunostained. Compared with WT controls, iTat mice showed increased GFAP expression, BiP expression, and loss of neuron dendrites in the brain when given Dox (Fig. 7, A and B). Compared with the PBS control, 4-PBA treatment slightly decreased GFAP expression and BiP expression in the brain of WT mice but considerably decreased GFAP expression, BiP expression, and loss of neuron dendrites in the brain of iTat mice. Taken together, these results show that ER stress is directly linked to astrocyte-mediated Tat neurotoxicity and suggest that alleviating ER stress could serve as a potential therapeutic strategy for HIV/neuroAIDS.

Discussion

In this study, we first showed that HIV-1 Tat-induced GFAP up-regulation led to GFAP aggregation and activated UPR/ER stress in astrocytes (Figs. 1–3 and supplemental Fig. S1). We

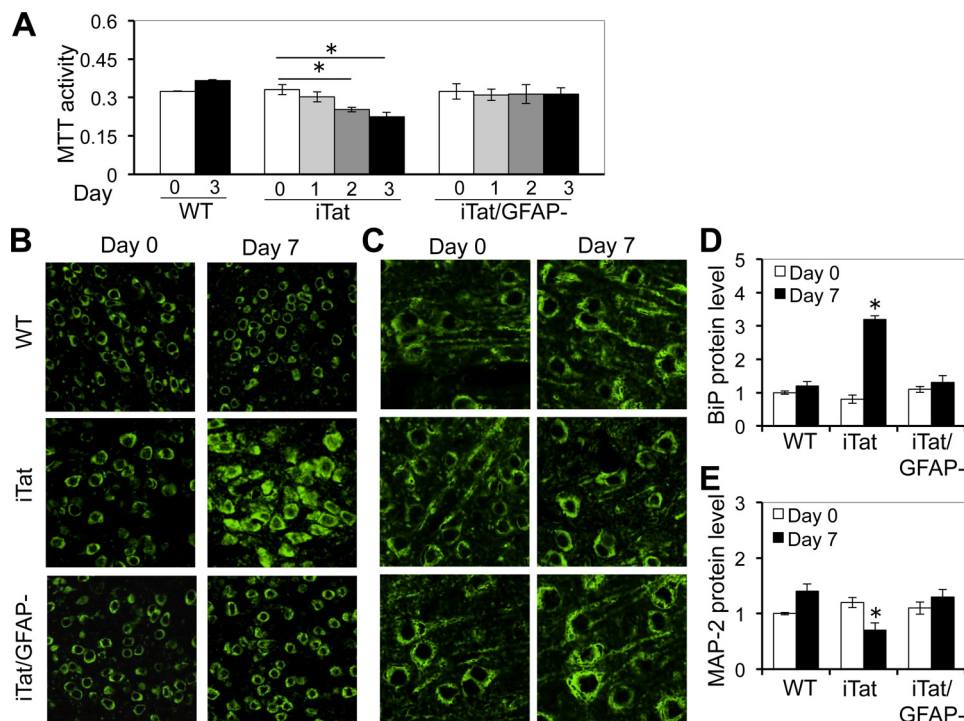


FIGURE 4. GFAP knock-out abolished Tat-induced astrocyte-mediated Tat neurotoxicity *in vitro* and ER stress in the brain. *A*, primary astrocytes were isolated from WT, iTat, or iTat/GFAP knock-out (iTat/GFAP⁻) mice and cultured in the presence of 5 μ g/ml Dox for the indicated days, and the culture supernatants were collected and assayed for their neurotoxicity in SH-SY5Y. The data are the mean \pm S.D. (error bars) of triplicates. *B–E*, WT, iTat, or iTat/GFAP⁻ mice (3 mice/strain) were injected i.p. with Dox (80 mg/kg/day) for 0 and 7 days. The brains were collected and sectioned, and comparable cortical sections were stained with an antibody for BiP (*B*) or MAP-2 (*C*), followed by goat anti-mouse Alexa Fluor 488. -Fold changes in BiP expression (*D*) or MAP-2 expression (*E*) over the control (WT at day 0) were the mean \pm S.D. of multiple cortical sections from each strain. *, $p < 0.05$.

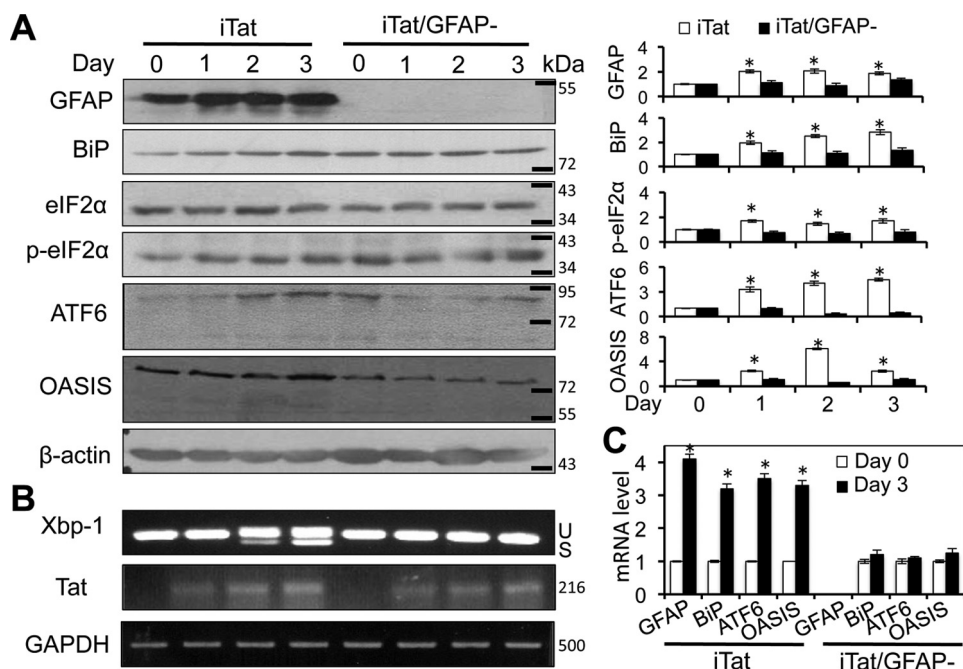


FIGURE 5. GFAP knock-out abolished Tat-induced ER stress in astrocytes *in vitro*. Primary astrocytes were isolated from iTat and iTat/GFAP⁻ mice; cultured in the presence of 5 μ g/ml Dox for 0, 1, 2, and 3 days; and then analyzed for GFAP, BiP, total eIF-2 α , phospho-eIF2 α (p-eIF-2 α), ATF6, and OASIS expression by Western blotting (*A*). -Fold changes in protein expression over day 0 were the mean \pm S.D. (error bars) of three independent repeats and are shown to the right of the respective Western blots. Total RNA was isolated from those cells for Xbp1 alternative splicing and Tat expression by semiquantitative RT-PCR (*B*). GAPDH was included as a control. *U* and *S*, unspliced and spliced RNA-derived PCR DNA, respectively. Total RNA was also analyzed for GFAP, BiP, ATF6, and OASIS mRNA expression by quantitative RT-PCR (*C*). β -Actin was included as an internal control. -Fold changes in mRNA expression over the control (day 0) were the mean \pm S.D. of three independent repeats. *, $p < 0.05$.

next demonstrated that GFAP expression was associated with Tat-induced UPR/ER stress in astrocytes and astrocyte-mediated Tat neurotoxicity (Figs. 4 and 5 and supplemental Fig. S3).

Furthermore, we demonstrated that inhibition of UPR/ER stress by the chemical chaperone 4-PBA alleviated astrocyte-mediated Tat neurotoxicity *in vitro* and *in vivo* (Figs. 6 and 7),

Tat Activation of UPR/ER Stress in Astrocytes

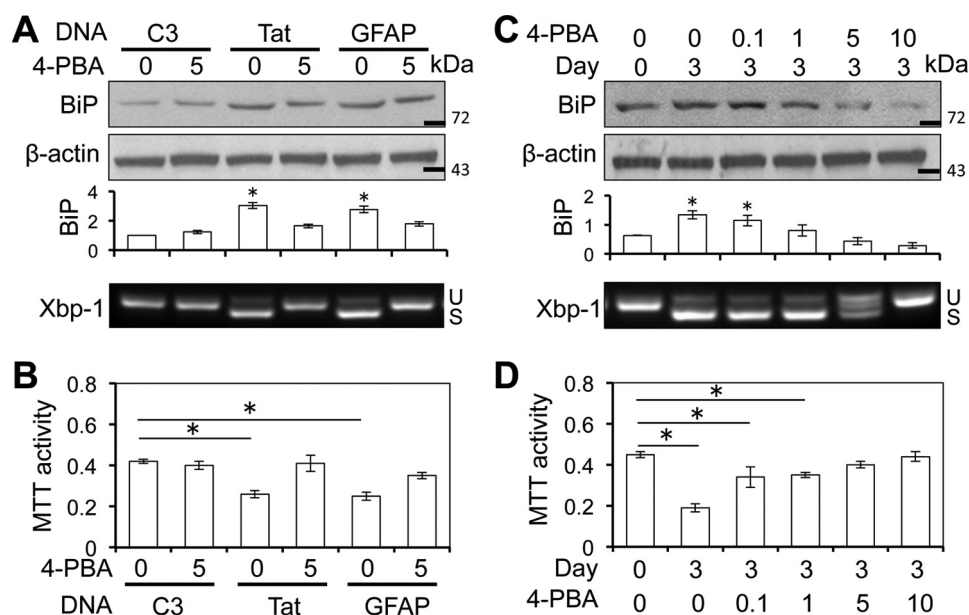


FIGURE 6. 4-PBA inhibited Tat-induced ER stress in astrocytes and astrocyte-mediated Tat neurotoxicity. *A* and *B*, U373.MG cells were transfected with cDNA3, Tat, or GFAP expression plasmid; cultured for 48 h; and continued to culture in the presence of 0 and 5 mM 4-PBA for 24 h. A fraction of the cells were harvested and analyzed for BiP expression by Western blotting, and total RNA was isolated from the remaining cells for Xbp-1 alternate splicing by semiquantitative RT-PCR (*A*). The culture supernatants from the 4-PBA-treated cells were evaluated for neurotoxicity using the MTT assay (*B*). *C* and *D*, iTat primary astrocytes were cultured in the presence of 5 μ g/ml Dox for 0 and 3 days and then in the presence of 0, 0.1, 1, 5, or 10 mM 4-PBA for 24 h. A fraction of the cells were harvested and analyzed for BiP expression by Western blotting, and total RNA was isolated from the remaining cells for Xbp-1 alternate splicing by semiquantitative RT-PCR (*C*). *U* and *S*, unspliced and spliced RNA-derived PCR DNA, respectively. The culture supernatants from the 4-PBA-treated cells were evaluated for neurotoxicity using the MTT assay (*D*). -Fold changes in BiP expression over the control (C3 at day 0) were the mean \pm S.D. (*error bars*) of three independent repeats and are shown *below* the respective Western blots (*A* and *C*). *, $p < 0.05$.

which might be considered as a potential therapeutic strategy in the treatment of HIV/neuroAIDS or other astrocytosis-related neurodegenerative diseases.

As an astrocyte marker, GFAP is a type III intermediate filament protein and is mainly located in cytoskeletal compartments (65). Its expression is developmentally and pathophysiologically regulated (for a review, see Ref. 66). GFAP has 432 amino acids and a molecular mass of 55 kDa and is considerably conserved among species (67). Like other cell type-specific intermediate filament proteins, GFAP forms extensive networks that maintain mechanical strength and shape of the astrocytes and provide dynamic platforms for the organization of the cytoplasm at a structural and functional level (68). Specifically, GFAP is involved in astrocyte volume regulation (69), glial scar formation (70), and anchoring glutamate transporters to the plasma membrane to facilitate neurotransmitter recycling (71). In addition, GFAP plays a critical role in neuron-glia interaction and CNS morphogenesis (72, 73). Recent findings suggest GFAP involvement in the long term maintenance of the brain architecture, proper function of the blood-brain barrier, and modulation of some neuronal functions (72, 74). Mutations in GFAP cause Alexander disease (50, 75), whereas higher levels of GFAP lead to premature death (49, 76). Interestingly, both cases are pathologically characterized by formation of cytoplasmic GFAP aggregates or inclusions (49, 50, 75, 77). Similar findings have been noted with other intermediate filament proteins, such as keratin and desmin (78, 79). Thus, we evaluated the effects of Tat-activated GFAP expression on the organization of GFAP filaments in astrocytes and found that Tat-activated GFAP expression led to the formation of GFAP aggregates and alteration of the intermediate filament network in astrocytes

(Fig. 1). These results provide the very first evidence to support the involvement of GFAP dysregulation in astrocyte-mediated Tat neurotoxicity.

Deposition of insoluble or misfolded protein aggregates in or around neurons is a common pathological feature of neurodegenerative diseases, such as Alzheimer disease, Parkinson disease, Huntington disease, Pelizaeus-Merzbacher disease, prion disease, and amyotrophic lateral sclerosis (50–53, 80). These aggregates are often cytotoxic and alter various cell signaling systems and neuron connectivity and cause neuron death through UPR and ER stress response (81, 82). Interestingly, ER stress activation has only recently been detected in HIV-induced neurodegeneration (56, 57). However, none of the neurodegenerative diseases have been linked to the formation of protein aggregates in astrocytes, specifically GFAP activation and aggregates and UPR/ER stress in astrocytes. In this study, we demonstrated that increased GFAP expression alone or in the presence of Tat expression activated all UPR/ER pathways, including PERK, IRE-1, ATF6, and OASIS (Figs. 1–3 and [supplemental Fig. S1](#)). These findings are indirectly supported by several early studies in the literature. Biochemical analyses have shown that ubiquitin and two small heat shock proteins (HSPs), α -B-crystallin and HSP27, are enriched in the GFAP aggregates resulting from higher levels of both wild-type GFAP expression and expression of GFAP mutants such as those in Alexander disease (83). cDNA microarray profiling of the GFAP transgenic mouse brain has also revealed gene expression patterns of a stress response (49, 84).

Astrocytes occupy about 20% of the cell volume of the gray matter and establish a highly dynamic reciprocal relationship with neurons that influence CNS growth, morphology, repair,

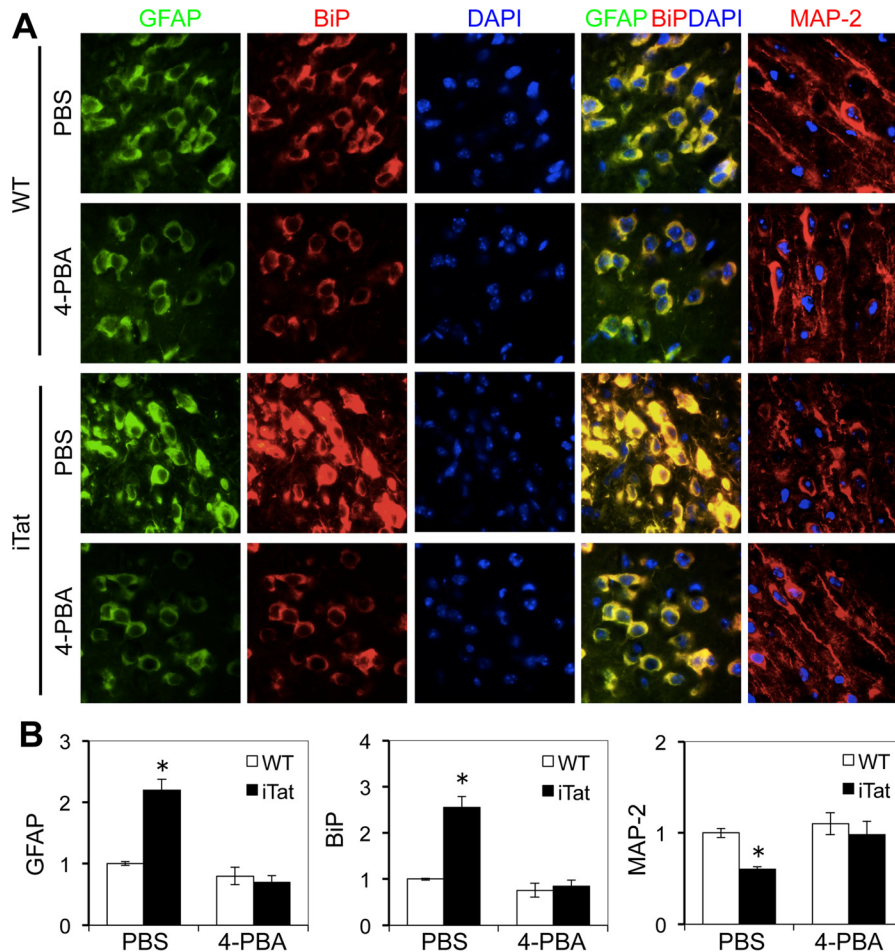


FIGURE 7. 4-PBA inhibited GFAP activation and formation of shortened neuron dendrites in the brain of iTat mice. WT and iTat mice (3 mice/strain) were injected i.p. with Dox (80 mg/kg/day) for 4 days and then with Dox (80 mg/kg/day) and 4-PBA (120 mg/kg/day) for an additional 3 days. The brains were collected 1 day after the final injection and sectioned, and comparable cortical sections were stained with an antibody for GFAP or BiP, followed by goat anti-rabbit Alexa Fluor 488 and goat anti-mouse Alexa Fluor 555, respectively. The sections were also counterstained with 100 ng/ml DAPI for nuclei. The images are representative of all of the stained cortical sections from each strain (A). -Fold changes in protein expression over the control (WT, -4-PBA) were the mean \pm S.D. (error bars) of multiple cortical sections from each strain (B). *, $p < 0.05$.

and aging and provide numerous targets for neurotoxic chemicals and disease processes as well as therapeutic drugs (35). Reactive astrocytes, or astrogliosis, characterized by increased GFAP expression, is one of the main characteristics of the astrocytic reaction commonly observed in CNS injury, as a result of either physical, pathological, or chemical insults (85), and is also the most common and consistent hallmark of HIV infection of the CNS, even in the era of combination of antiretroviral therapy (86, 87). Deletion and ectopic expression of GFAP (73, 77), expression of GFAP mutants (50, 59), and increased GFAP expression as shown in the context of Tat expression in this study and our previous studies (40, 46–48, 58) all point to the utmost importance of maintaining an empirical level of GFAP expression for normal function of astrocytes. Thus, the findings from the current study strongly suggest that aberrant astrogliosis/GFAP up-regulation actively contributes to neurodegenerative diseases. In addition, we showed in the study that blocking ER stress with chemical chaperone 4-PBA relieved astrocyte-mediated Tat neurotoxicity both *in vitro* and *in vivo* (Figs. 6 and 7). These results further validate the roles of GFAP activation-induced UPR/ER stress in astrocyte-mediated

Tat neurotoxicity and confirm the roles of astrocytes in HIV/neuroAIDS and other neurodegenerative diseases. Moreover, these results provide a new strategy for development of therapeutics targeted at HIV/neuroAIDS and other astrogliosis-related neurodegenerative diseases.

Materials and Methods

Animals and Tissues—C57BL/6 mice were purchased from the Jackson Laboratory (Bar Harbor, ME). Doxycycline (Dox)-inducible and astrocyte-specific HIV-1 Tat-transgenic mice (iTat) were created in our laboratory as described previously (58). GFAP-null mice were generously provided by Dr. Albee Messing (University of Wisconsin, Madison, WI) (72). iTat/GFAP-null (iTat/GFAP^{-/-}) mice were obtained by cross-breeding iTat mice with GFAP-null mice and characterized as described previously (88). For Tat induction, iTat mice were injected i.p. with Dox (Sigma) for 7 days (58). For 4-PBA (Sigma) treatment, mice were first injected i.p. with Dox for 4 days and then injected with Dox and 4-PBA (120 mg/kg) at 1-h intervals for 3 days. Then the mouse brain was collected 1 day after the final injection (64). Dox dosage was maintained at (80 mg/kg/day) for all experiments. Cortical brain tissues from HIV-

Tat Activation of UPR/ER Stress in Astrocytes

seronegative and HIV-infected and -demented subjects were kindly provided by Dr. Susan Morgello (Mount Sinai School of Medicine, New York) through the National NeuroAIDS Tissue Consortium.

Cells and Cell Cultures—Human astrocytoma U373.MG and human neuroblastoma SH-SY5Y were purchased from American Tissue Culture Collection (Manassas, VA). U373.MG cells were cultured in DMEM, whereas SH-SY5Y cells were cultured in 50% DMEM and 50% F-12 medium (Cellgro, Manassas, VA). Both culture media were supplemented with 10% FBS, 50 units/ml penicillin, and 50 μ g/ml streptomycin. Mouse primary astrocytes were isolated from the brain of embryonic day 18.5 embryos and induced to express Tat as described previously (40). Human primary fetal astrocytes were prepared as described (89). Primary astrocytes were cultured in F12-K medium (Cellgro) containing 10% FBS, 50 units/ml penicillin, and 50 μ g/ml streptomycin and passaged every 3–4 days.

Plasmids and Transfection—Plasmid pcDNA3 was purchased from Clontech (Mountain View, CA). Plasmids pGFAP-HA (46–48) and pTat.Myc (90) were constructed as described previously. Plasmid pHGFAP (R239H) was kindly provided by Dr. Michael Brenner (University of Alabama, Birmingham, AL); it expressed a human mutant GFAP with a change of amino acid residue at 239 from arginine to histidine. All cell transfections were performed using the standard calcium phosphate precipitation method.

Western Blotting—Cells were washed twice with ice-cold PBS and lysed in RIPA buffer (50 mM Tris·HCl, pH 7.4, 150 mM NaCl, 1% Triton X-100, 1% sodium deoxycholate, 0.1% SDS, 2 mM PMSE, and 1 \times protease inhibitor mixture (Roche Applied Science)) on ice for 20 min for whole cell lysates. Protein concentration of the cell lysates was determined using a Bio-Rad DC protein assay kit. Cell lysates were electrophoretically separated by 10% SDS-polyacrylamide gel, followed by probing with appropriate primary and secondary antibodies, ECL detection, and imaging using a Bio-Rad ChemicDoc imaging system (Bio-Rad). Mouse monoclonal α -GFAP (catalog no. AB5804), α - β -actin antibodies (catalog no. A2228), and α -CREB3L1 (catalog no. AV39769; for OASIS detection) were from Sigma; rabbit polyclonal α -eIF-1 α (catalog no. 9722) and goat polyclonal α -phospho-eIF-1 α (catalog no. 9721) were from Cell Signaling (Danvers, MA); rabbit polyclonal α -ATF6 (catalog no. IMG-273) was from IMGENEX (San Diego, CA); mouse monoclonal α -KDEL (catalog no. SPA-827) was from Assay Designs (Ann Arbor, MI); rabbit polyclonal α -GFAP (catalog no. Z0334) was from Dako (Carpinteria, CA); and rabbit polyclonal α -Myc (catalog no. sc-789) and mouse monoclonal α -MAP-2 (catalog no. sc-32791) were from Santa Cruz Biotechnology, Inc. (Dallas, TX).

RNA Isolation, Semiquantitative RT-PCR, and Quantitative RT-PCR—Total RNA was isolated using a TRIzol reagent kit (Invitrogen) according to the manufacturer's instructions. RT-PCR was performed on a PE Thermocycler 9700 (PerkinElmer Life Sciences) using a Titan One Tube RT-PCR kit (Roche Applied Science). RT-PCR primers and programs for Tat were as follows: 5'-GTC GGG ATC CTA ATG GAG CCA GTA GAT CCT-3' and 5'-TGC TTT GAT AGA GAA ACT TGA TGA GTC-3' and a program of 50 °C for 30 min, 94 °C for 3

min, followed by 30 cycles of 94 °C for 1 min, 50 °C for 30 s, and 72 °C for 45 s and one cycle of 72 °C for 5 min; for GFAP: 5'-AAG CAG ATG AAG CCA CCC TG-3' and 5'-GTC TGC ACG GGA ATG GTG AT-3' and a program of 50 °C for 30 min, 94 °C for 3 min, followed by 25 cycles of 94 °C for 1 min, 52 °C for 1 min, and 68 °C for 1 min and one cycle of 68 °C for 7 min; for human Xbp-1 alternate spliced transcripts: 5'-TTA CGA GAG AAA ACT CAT GGC-3' and 5'-GGG TCC AAG TTG TCC AGA ATG C-3'; for mouse Xbp-1 alternate spliced transcripts: 5'-TTA CGG GAG AAA ACT CAC GGC-3' and 5'-GGG TCC AAC TTG TCC AGA ATG-3' and a program of 50 °C for 30 min, 95 °C for 3 min, followed by 35 cycles of 95 °C for 1 min, 58 °C for 30 s, and 72 °C for 30 s and one cycle of 72 °C for 5 min.

For quantitative RT-PCR, cDNAs were synthesized and used for SYBR Green quantitative PCR (Thermo Fisher Scientific) with a program of 50 °C for 30 min, 95 °C for 3 min, followed by 35 cycles of 95 °C for 1 min, 58 °C for 30 s, and 72 °C for 30 s and one cycle of 72 °C for 5 min. Primers were as follows: 5'-TCT AAG TTT GCA GAC CTC ACA GA-3' and 5'-ACT CCA GAT CGC AGG TCA A-3' for GFAP; 5'-GCA TGA TGA AGT TCA CTG TGG-3' and 5'-CAC ACC GAC GCA GGA ATA-3' for BiP; 5'-GCT TGC AAA CAC AGG AAA GA-3' and 5'-CCC AGA GGA AGT CAC TCC A-3' for ATF6; and 5'-TGA GCT GTG GAA GAA AGT GG-3' and 5'-GGT CTG GAG ATC TTG CTG GT-3' for OASIS.

Immunofluorescence Staining—Mouse primary astrocytes were cultured on a polylysine-coated coverslip (Sigma) in the presence of Dox for indicated lengths of time. The cells were washed with ice-cold PBS; fixed in 4% paraformaldehyde for 30 min; permeabilized in 0.5% Triton-X 100 for 30 min; and blocked in 5% BSA, 1% nonfat milk, and 0.3% Triton X-100 for 1 h. Following blocking, the cells were stained with mouse monoclonal anti-GFAP (1:200) at 4 °C overnight and then goat anti-mouse secondary antibody Alexa Fluor 555 (1:500) at room temperature for 1 h. The nuclei of the cells were counterstained with 0.1 μ g/ml DAPI. Extensive washes with PBS were performed between steps. Omission of the primary antibody in parallel staining was included as a control to ensure no nonspecific staining.

For mouse and human brain tissues, paraffin-embedded sections (8 μ m) were prepared and placed on slides and deparaffinized in xylene twice, each for 10 min, and rehydrated in decreasing concentrations of ethanol (100, 95, and 70%), each for 10 min. The tissue slides were placed in the target retrieval solution (Dako) and treated at 95 °C for 40 min. After cooling to the room temperature, the tissues were permeabilized in 0.2% Triton X-100 for 10 min and incubated in 0.3% H₂O₂ for 30 min. The immunostaining was performed using a tyramide signal amplification kit according to the manufacturer's instructions (Invitrogen). For GFAP or BiP single staining, the tissues were stained with mouse anti-GFAP or mouse anti-KDEL antibody plus goat anti-mouse HRP followed by tyramide signal amplification. For GFAP and BiP double staining, the tissues were stained with rabbit anti-GFAP antibody (Dako) plus goat anti-rabbit HRP followed by tyramide signal amplification and then with mouse anti-KDEL followed by bovine anti-goat Alexa

Fluor 555. The images were captured using an Olympus 2 microscope with a $\times 60$ objective.

3-(4,5-Dimethylthiazol-2-yl)-2,5-diphenyl Tetrazolium Bromide (MTT) Assay—The neurotoxicity of the astrocyte culture supernatants was determined in SH-SY5Y or human primary neurons using the MTT assay. Human primary neurons or SH-SY5Y cells were plated in a 48-well plate at a density of 1×10^5 cells/well and cultured for 2 days. The cells were exposed to culture supernatants (2:1 ratio) collected from astrocytes that were either transfected with plasmids or induced with Dox and continued to culture for an additional 3 days. MTT (5 mg/ml) was added directly to the culture medium to a final concentration of 1 mg/ml, and the cultures were incubated at 37 °C for 4 h. The medium was then removed, and the purple crystal precipitates were dissolved in 200 μ l of acid-isopropyl alcohol (44 ml of isopropyl alcohol plus 6 ml of 0.2 N HCl). Aliquots of the acid-isopropyl alcohol solvent were transferred into the wells of a 96-well plate, and the optical density was determined using a microplate reader at a test wavelength of 490 nm and a reference wavelength of 650 nm and then used to represent the relative cell viability.

Data Acquisition and Analysis—The protein levels on Western blots were quantitated using ImageJ (National Institutes of Health), normalized to β -actin, except for phosphorylated eIF-2 α , which was normalized to total eIF-2 α , and calculated as -fold changes over the control. The protein levels upon immunofluorescence staining of human or mouse brain tissues were quantitated using ImageJ, divided by the number of nuclei, and calculated as -fold changes over the control. The data are representative of three or more independent repeats. All experimental data were analyzed by two-tailed Student's *t* test. A *p* value of <0.05 was considered to be statistically significant and shown as an asterisk; a *p* value of <0.01 was considered to be statistically highly significant and shown as a double asterisk.

Author Contributions—Y. F. conducted and designed the experiments and prepared the data and the draft, and J. J. H. designed the experiments, prepared the data, and wrote the manuscript.

Acknowledgments—We thank Dr. Albee Messing for the GFAP-null mice, Dr. Michael Brenner for the pGFAP R239H plasmid, and Dr. Susan Morgallo for the human brain tissues. We also thank Dr. Linden Green for technical assistance and Dr. Pejman Rahimain and Amanda Whitmill for critical reading of the manuscript.

References

- Kaul, M., Garden, G. A., and Lipton, S. A. (2001) Pathways to neuronal injury and apoptosis in HIV-associated dementia. *Nature* **410**, 988–994
- Kaul, M., Zheng, J., Okamoto, S., Gendelman, H. E., and Lipton, S. A. (2005) HIV-1 infection and AIDS: consequences for the central nervous system. *Cell Death Differ.* **12**, 878–892
- Ellis, R. J., Deutsch, R., Heaton, R. K., Marcotte, T. D., McCutchan, J. A., Nelson, J. A., Abramson, I., Thal, L. J., Atkinson, J. H., Wallace, M. R., and Grant, I. (1997) Neurocognitive impairment is an independent risk factor for death in HIV infection. San Diego HIV Neurobehavioral Research Center Group. *Arch. Neurol.* **54**, 416–424
- Ellis, R., Langford, D., and Masliah, E. (2007) HIV and antiretroviral therapy in the brain: neuronal injury and repair. *Nat. Rev. Neurosci.* **8**, 33–44
- Burdo, T. H., Lackner, A., and Williams, K. C. (2013) Monocyte/macrophages and their role in HIV neuropathogenesis. *Immunol. Rev.* **254**, 102–113
- Irish, B. P., Khan, Z. K., Jain, P., Nonnemacher, M. R., Pirrone, V., Rahman, S., Rajagopalan, N., Suchitra, J. B., Mostoller, K., and Wigdahl, B. (2009) Molecular mechanisms of neurodegenerative diseases induced by human retroviruses: a review. *Am. J. Infect. Dis.* **5**, 231–258
- Kruman, I. I., Nath, A., and Mattson, M. P. (1998) HIV-1 protein Tat induces apoptosis of hippocampal neurons by a mechanism involving caspase activation, calcium overload, and oxidative stress. *Exp. Neurol.* **154**, 276–288
- Shi, B., Raina, J., Lorenzo, A., Busciglio, J., and Gabuzda, D. (1998) Neuronal apoptosis induced by HIV-1 Tat protein and TNF- α : potentiation of neurotoxicity mediated by oxidative stress and implications for HIV-1 dementia. *J. Neurovirol.* **4**, 281–290
- Gavriil, E. S., Cooney, R., and Weeks, B. S. (2000) Tat mediates apoptosis in vivo in the rat central nervous system. *Biochem. Biophys. Res. Commun.* **267**, 252–256
- New, D. R., Maggirwar, S. B., Epstein, L. G., Dewhurst, S., and Gelbard, H. A. (1998) HIV-1 Tat induces neuronal death via tumor necrosis factor- α and activation of non-N-methyl-D-aspartate receptors by a NF κ B-independent mechanism. *J. Biol. Chem.* **273**, 17852–17858
- Frankel, A. D., and Pabo, C. O. (1988) Cellular uptake of the tat protein from human immunodeficiency virus. *Cell* **55**, 1189–1193
- Helland, D. E., Welles, J. L., Caputo, A., and Haseltine, W. A. (1991) Transcellular transactivation by the human immunodeficiency virus type 1 tat protein. *J. Virol.* **65**, 4547–4549
- Liu, Y., Jones, M., Hingtgen, C. M., Bu, G., Larabee, N., Tanzi, R. E., Moir, R. D., Nath, A., and He, J. J. (2000) Uptake of HIV-1 tat protein mediated by low-density lipoprotein receptor-related protein disrupts the neuronal metabolic balance of the receptor ligands. *Nat. Med.* **6**, 1380–1387
- Apra, S., Del Valle, L., Mameli, G., Sawaya, B. E., Khalili, K., and Peruzzi, F. (2006) Tubulin-mediated binding of human immunodeficiency virus-1 Tat to the cytoskeleton causes proteasomal-dependent degradation of microtubule-associated protein 2 and neuronal damage. *J. Neurosci.* **26**, 4054–4062
- Caporello, E., Nath, A., Slevin, J., Galey, D., Hamilton, G., Williams, L., Steiner, J. P., and Haughey, N. J. (2006) The immunophilin ligand GPI1046 protects neurons from the lethal effects of the HIV-1 proteins gp120 and Tat by modulating endoplasmic reticulum calcium load. *J. Neurochem.* **98**, 146–155
- Norman, J. P., Perry, S. W., Kasischke, K. A., Volsky, D. J., and Gelbard, H. A. (2007) HIV-1 trans activator of transcription protein elicits mitochondrial hyperpolarization and respiratory deficit, with dysregulation of complex IV and nicotinamide adenine dinucleotide homeostasis in cortical neurons. *J. Immunol.* **178**, 869–876
- Jones, M., Olafson, K., Del Bigio, M. R., Peeling, J., and Nath, A. (1998) Intraventricular injection of human immunodeficiency virus type 1 (HIV-1) tat protein causes inflammation, gliosis, apoptosis, and ventricular enlargement. *J. Neuropathol. Exp. Neurol.* **57**, 563–570
- Benelli, R., Barbero, A., Ferrini, S., Scapini, P., Cassatella, M., Bussolino, F., Tacchetti, C., Noonan, D. M., and Albin, A. (2000) Human immunodeficiency virus transactivator protein (Tat) stimulates chemotaxis, calcium mobilization, and activation of human polymorphonuclear leukocytes: implications for Tat-mediated pathogenesis. *J. Infect. Dis.* **182**, 1643–1651
- de Paulis, A., De Palma, R., Di Gioia, L., Carfora, M., Prevete, N., Tosi, G., Accolla, R. S., and Marone, G. (2000) Tat protein is an HIV-1-encoded β -chemokine homolog that promotes migration and up-regulates CCR3 expression on human Fc ϵ RI+ cells. *J. Immunol.* **165**, 7171–7179
- Park, I. W., Wang, J. F., and Groopman, J. E. (2001) HIV-1 Tat promotes monocyte chemoattractant protein-1 secretion followed by transmigration of monocytes. *Blood* **97**, 352–358
- Albin, A., Soldi, R., Giunciuglio, D., Giraudo, E., Benelli, R., Primo, L., Noonan, D., Salio, M., Camussi, G., Rockl, W., and Bussolino, F. (1996) The angiogenesis induced by HIV-1 tat protein is mediated by the Flk-1/KDR receptor on vascular endothelial cells. *Nat. Med.* **2**, 1371–1375
- Eugenin, E. A., King, J. E., Nath, A., Calderon, T. M., Zukin, R. S., Bennett, M. V., and Berman, J. W. (2007) HIV-tat induces formation of an LRP-

Tat Activation of UPR/ER Stress in Astrocytes

- PSD-95- NMDAR-nNOS complex that promotes apoptosis in neurons and astrocytes. *Proc. Natl. Acad. Sci. U.S.A.* **104**, 3438–3443
23. Peruzzi, F. (2006) The multiple functions of HIV-1 Tat: proliferation versus apoptosis. *Front. Biosci.* **11**, 708–717
24. Brack-Werner, R. (1999) Astrocytes: HIV cellular reservoirs and important participants in neuropathogenesis. *AIDS* **13**, 1–22
25. Tornatore, C., Chandra, R., Berger, J. R., and Major, E. O. (1994) HIV-1 infection of subcortical astrocytes in the pediatric central nervous system. *Neurology* **44**, 481–487
26. Gorry, P. R., Ong, C., Thorpe, J., Bannwarth, S., Thompson, K. A., Gatignol, A., Vesselingh, S. L., and Purcell, D. F. (2003) Astrocyte infection by HIV-1: mechanisms of restricted virus replication, and role in the pathogenesis of HIV-1-associated dementia. *Curr. HIV Res.* **1**, 463–473
27. Saito, Y., Sharer, L. R., Epstein, L. G., Michaels, J., Mintz, M., Louder, M., Golding, K., Cvetkovich, T. A., and Blumberg, B. M. (1994) Overexpression of nef as a marker for restricted HIV-1 infection of astrocytes in postmortem pediatric central nervous tissues. *Neurology* **44**, 474–481
28. Messam, C. A., and Major, E. O. (2000) Stages of restricted HIV-1 infection in astrocyte cultures derived from human fetal brain tissue. *J. Neurovirol.* **6**, S90–S94
29. Bagasra, O., Lavi, E., Bobroski, L., Khalili, K., Pestaner, J. P., Tawadros, R., and Pomerantz, R. J. (1996) Cellular reservoirs of HIV-1 in the central nervous system of infected individuals: identification by the combination of *in situ* polymerase chain reaction and immunohistochemistry. *AIDS* **10**, 573–585
30. Blum, A. L., and Hollender, L. F. (1979) [Management of peptic ulcer: internistically or surgically?]. *Internist* **20**, 162–166
31. Sabri, F., Tresoldi, E., Di Stefano, M., Polo, S., Monaco, M. C., Verani, A., Fiore, J. R., Lusso, P., Major, E., Chiodi, F., and Scarlatti, G. (1999) Non-productive human immunodeficiency virus type 1 infection of human fetal astrocytes: independence from CD4 and major chemokine receptors. *Virology* **264**, 370–384
32. Williams, K. C., and Hickey, W. F. (1996) Traffic of lymphocytes into the CNS during inflammation and HIV infection. *J. NeuroAIDS* **1**, 31–55
33. Nottet, H. S., Persidsky, Y., Sasseville, V. G., Nukuna, A. N., Bock, P., Zhai, Q. H., Sharer, L. R., McComb, R. D., Swindells, S., Soderland, C., and Gendelman, H. E. (1996) Mechanisms for the transendothelial migration of HIV-1-infected monocytes into brain. *J. Immunol.* **156**, 1284–1295
34. Yuen, K. Y., Chan, K. S., Chan, C. M., Ho, P. L., and Ng, M. H. (1997) Monitoring the therapy of pulmonary tuberculosis by nested polymerase chain reaction assay. *J. Infect.* **34**, 29–33
35. Eddleston, M., and Mucke, L. (1993) Molecular profile of reactive astrocytes: implications for their role in neurologic disease. *Neuroscience* **54**, 15–36
36. Mennerick, S., and Zorumski, C. F. (1994) Glial contributions to excitatory neurotransmission in cultured hippocampal cells. *Nature* **368**, 59–62
37. Charles, A. C., Merrill, J. E., Dirksen, E. R., and Sanderson, M. J. (1991) Intercellular signaling in glial cells: calcium waves and oscillations in response to mechanical stimulation and glutamate. *Neuron* **6**, 983–992
38. Conant, K., Garzino-Demo, A., Nath, A., McArthur, J. C., Halliday, W., Power, C., Gallo, R. C., and Major, E. O. (1998) Induction of monocyte chemoattractant protein-1 in HIV-1 Tat-stimulated astrocytes and elevation in AIDS dementia. *Proc. Natl. Acad. Sci. U.S.A.* **95**, 3117–3121
39. Vitkovic, L., Chatham, J. J., and da Cunha, A. (1995) Distinct expressions of three cytokines by IL-1-stimulated astrocytes *in vitro* and in AIDS brain. *Brain Behav. Immun.* **9**, 378–388
40. Zhou, B. Y., Liu, Y., Kim, B. O., Xiao, Y., and He, J. J. (2004) Astrocyte activation and dysfunction and neuron death by HIV-1 Tat expression in astrocytes. *Mol. Cell. Neurosci.* **27**, 296–305
41. Speth, C., Schabetsberger, T., Mohsenipour, I., Stöckl, G., Würzner, R., Stoiber, H., Lass-Flörl, C., and Dierich, M. P. (2002) Mechanism of human immunodeficiency virus-induced complement expression in astrocytes and neurons. *J. Virol.* **76**, 3179–3188
42. Ton, H., and Xiong, H. (2013) Astrocyte dysfunctions and HIV-1 neurotoxicity. *J. AIDS Clin. Res.* **4**, 255
43. Deshpande, M., Zheng, J., Borgmann, K., Persidsky, R., Wu, L., Schellpeper, C., and Ghorpade, A. (2005) Role of activated astrocytes in neuronal damage: potential links to HIV-1-associated dementia. *Neurotox. Res.* **7**, 183–192
44. Tewari, M., Varghse, R. K., Menon, M., and Seth, P. (2015) Astrocytes mediate HIV-1 Tat-induced neuronal damage via ligand-gated ion channel P2X7R. *J. Neurochem.* **132**, 464–476
45. Zhou, B. Y., and He, J. J. (2004) Proliferation inhibition of astrocytes, neurons, and non-glia cells by intracellularly expressed human immunodeficiency virus type 1 (HIV-1) Tat protein. *Neurosci. Lett.* **359**, 155–158
46. Zou, W., Wang, Z., Liu, Y., Fan, Y., Zhou, B. Y., Yang, X. F., and He, J. J. (2010) Involvement of p300 in constitutive and HIV-1 Tat-activated expression of glial fibrillary acidic protein in astrocytes. *Glia* **58**, 1640–1648
47. Fan, Y., Zou, W., Green, L. A., Kim, B. O., and He, J. J. (2011) Activation of Egr-1 expression in astrocytes by HIV-1 Tat: new insights into astrocyte-mediated Tat neurotoxicity. *J. Neuroimmune Pharmacol.* **6**, 121–129
48. Fan, Y., Timani, K. A., and He, J. J. (2015) STAT3 and its phosphorylation are involved in HIV-1 Tat-induced transactivation of glial fibrillary acidic protein. *Curr. HIV Res.* **13**, 55–63
49. Tanaka, K. F., Takebayashi, H., Yamazaki, Y., Ono, K., Naruse, M., Iwasato, T., Itohara, S., Kato, H., and Ikenaka, K. (2007) Murine model of Alexander disease: analysis of GFAP aggregate formation and its pathological significance. *Glia* **55**, 617–631
50. Brenner, M., Johnson, A. B., Boespflug-Tanguy, O., Rodriguez, D., Goldman, J. E., and Messing, A. (2001) Mutations in GFAP, encoding glial fibrillary acidic protein, are associated with Alexander disease. *Nat. Genet.* **27**, 117–120
51. Cho, K. J., Lee, B. I., Cheon, S. Y., Kim, H. W., Kim, H. J., and Kim, G. W. (2009) Inhibition of apoptosis signal-regulating kinase 1 reduces endoplasmic reticulum stress and nuclear huntingtin fragments in a mouse model of Huntington disease. *Neuroscience* **163**, 1128–1134
52. Chigurupati, S., Wei, Z., Belal, C., Vandermeij, M., Kyriazis, G. A., Arumugam, T. V., and Chan, S. L. (2009) The homocysteine-inducible endoplasmic reticulum stress protein counteracts calcium store depletion and induction of CCAAT enhancer-binding protein homologous protein in a neurotoxin model of Parkinson disease. *J. Biol. Chem.* **284**, 18323–18333
53. Hoozemans, J. J., Veerhuis, R., Van Haastert, E. S., Rozemuller, J. M., Baas, F., Eikelenboom, P., and Scheper, W. (2005) The unfolded protein response is activated in Alzheimer's disease. *Acta Neuropathol.* **110**, 165–172
54. Harding, H. P., Zhang, Y., and Ron, D. (1999) Protein translation and folding are coupled by an endoplasmic-reticulum-resident kinase. *Nature* **397**, 271–274
55. Tirasophon, W., Welihinda, A. A., and Kaufman, R. J. (1998) A stress response pathway from the endoplasmic reticulum to the nucleus requires a novel bifunctional protein kinase/endoribonuclease (Ire1p) in mammalian cells. *Genes Dev.* **12**, 1812–1824
56. Akay, C., Lindl, K. A., Shyam, N., Nabet, B., Goenaga-Vazquez, Y., Ruzbarsky, J., Wang, Y., Kolson, D. L., and Jordan-Sciutto, K. L. (2012) Activation status of integrated stress response pathways in neurons and astrocytes of HIV-associated neurocognitive disorders (HAND) cortex. *Neuropathol. Appl. Neurobiol.* **38**, 175–200
57. Lindl, K. A., Akay, C., Wang, Y., White, M. G., and Jordan-Sciutto, K. L. (2007) Expression of the endoplasmic reticulum stress response marker, BiP, in the central nervous system of HIV-positive individuals. *Neuropathol. Appl. Neurobiol.* **33**, 658–669
58. Kim, B. O., Liu, Y., Ruan, Y., Xu, Z. C., Schantz, L., and He, J. J. (2003) Neuropathologies in transgenic mice expressing human immunodeficiency virus type 1 Tat protein under the regulation of the astrocyte-specific glial fibrillary acidic protein promoter and doxycycline. *Am. J. Pathol.* **162**, 1693–1707
59. Rodriguez, D., Gauthier, F., Bertini, E., Bugiani, M., Brenner, M., N'guyen, S., Goizet, C., Gelot, A., Surtees, R., Pedespan, J. M., Hernandezorena, X., Troncoso, M., Uziel, G., Messing, A., Ponsot, G., et al. (2001) Infantile Alexander disease: spectrum of GFAP mutations and genotype-phenotype correlation. *Am. J. Hum. Genet.* **69**, 1134–1140
60. Kondo, S., Murakami, T., Tatsumi, K., Ogata, M., Kanemoto, S., Otori, K., Iseki, K., Wanaka, A., and Imaizumi, K. (2005) OASIS, a CREB/ATF-family member, modulates UPR signalling in astrocytes. *Nat. Cell Biol.* **7**, 186–194

61. Dash, P. K., Gorantla, S., Gendelman, H. E., Knibbe, J., Casale, G. P., Markarov, E., Epstein, A. A., Gelbard, H. A., Boska, M. D., and Poluektova, L. Y. (2011) Loss of neuronal integrity during progressive HIV-1 infection of humanized mice. *J. Neurosci.* **31**, 3148–3157
62. Valero, I. P., Baeza, A. G., Hernandez-Tamames, J. A., Monge, S., Arnalich, F., and Arribas, J. R. (2014) Cerebral volumes, neuronal integrity and brain inflammation measured by MRI in patients receiving PI monotherapy or triple therapy. *J. Int. AIDS Soc.* **17**, 19578
63. Mimori, S., Okuma, Y., Kaneko, M., Kawada, K., Hosoi, T., Ozawa, K., Nomura, Y., and Hamana, H. (2012) Protective effects of 4-phenylbutyrate derivatives on the neuronal cell death and endoplasmic reticulum stress. *Biol. Pharm. Bull.* **35**, 84–90
64. Qi, X., Hosoi, T., Okuma, Y., Kaneko, M., and Nomura, Y. (2004) Sodium 4-phenylbutyrate protects against cerebral ischemic injury. *Mol. Pharmacol.* **66**, 899–908
65. Fuchs, E., and Weber, K. (1994) Intermediate filaments: structure, dynamics, function, and disease. *Annu. Rev. Biochem.* **63**, 345–382
66. Chiu, F. C., and Goldman, J. E. (1985) Regulation of glial fibrillary acidic protein (GFAP) expression in CNS development and in pathological states. *J. Neuroimmunol.* **8**, 283–292
67. Reeves, S. A., Helman, L. J., Allison, A., and Israel, M. A. (1989) Molecular cloning and primary structure of human glial fibrillary acidic protein. *Proc. Natl. Acad. Sci. U.S.A.* **86**, 5178–5182
68. Coulombe, P. A., and Wong, P. (2004) Cytoplasmic intermediate filaments revealed as dynamic and multipurpose scaffolds. *Nat. Cell Biol.* **6**, 699–706
69. Ding, M., Eliasson, C., Betsholtz, C., Hamberger, A., and Pekny, M. (1998) Altered taurine release following hypotonic stress in astrocytes from mice deficient for GFAP and vimentin. *Brain Res. Mol. Brain Res.* **62**, 77–81
70. Pekny, M., Johansson, C. B., Eliasson, C., Stakeberg, J., Wallén, A., Perlmann, T., Lendahl, U., Betsholtz, C., Berthold, C. H., and Frisén, J. (1999) Abnormal reaction to central nervous system injury in mice lacking glial fibrillary acidic protein and vimentin. *J. Cell Biol.* **145**, 503–514
71. Sullivan, S. M., Lee, A., Björkman, S. T., Miller, S. M., Sullivan, R. K., Poronnik, P., Colditz, P. B., and Pow, D. V. (2007) Cytoskeletal anchoring of GLAST determines susceptibility to brain damage: an identified role for GFAP. *J. Biol. Chem.* **282**, 29414–29423
72. McCall, M. A., Gregg, R. G., Behringer, R. R., Brenner, M., Delaney, C. L., Galbreath, E. J., Zhang, C. L., Pearce, R. A., Chiu, S. Y., and Messing, A. (1996) Targeted deletion in astrocyte intermediate filament (*Gfap*) alters neuronal physiology. *Proc. Natl. Acad. Sci. U.S.A.* **93**, 6361–6366
73. Pekny, M. (2001) Astrocytic intermediate filaments: lessons from GFAP and vimentin knock-out mice. *Prog. Brain Res.* **132**, 23–30
74. Liedtke, W., Edelmann, W., Bieri, P. L., Chiu, F. C., Cowan, N. J., Kuchelapati, R., and Raine, C. S. (1996) GFAP is necessary for the integrity of CNS white matter architecture and long-term maintenance of myelination. *Neuron* **17**, 607–615
75. Mignot, C., Boespflug-Tanguy, O., Gelot, A., Dautigny, A., Pham-Dinh, D., and Rodriguez, D. (2004) Alexander disease: putative mechanisms of an astrocytic encephalopathy. *Cell Mol. Life Sci.* **61**, 369–385
76. Messing, A. (1998) Transgenic studies of peripheral and central glia. *Int. J. Dev. Biol.* **42**, 1019–1024
77. Messing, A., Head, M. W., Galles, K., Galbreath, E. J., Goldman, J. E., and Brenner, M. (1998) Fatal encephalopathy with astrocyte inclusions in GFAP transgenic mice. *Am. J. Pathol.* **152**, 391–398
78. Bär, H., Fischer, D., Goudeau, B., Kley, R. A., Clemen, C. S., Vicart, P., Herrmann, H., Vorgerd, M., and Schröder, R. (2005) Pathogenic effects of a novel heterozygous R350P desmin mutation on the assembly of desmin intermediate filaments *in vivo* and *in vitro*. *Hum. Mol. Genet.* **14**, 1251–1260
79. Vassar, R., Coulombe, P. A., Degenstein, L., Albers, K., and Fuchs, E. (1991) Mutant keratin expression in transgenic mice causes marked abnormalities resembling a human genetic skin disease. *Cell* **64**, 365–380
80. Castilla, J., Hetz, C., and Soto, C. (2004) Molecular mechanisms of neurotoxicity of pathological prion protein. *Curr. Mol. Med.* **4**, 397–403
81. Bucciantini, M., Giannoni, E., Chiti, F., Baroni, F., Formigli, L., Zurdo, J., Taddei, N., Ramponi, G., Dobson, C. M., and Stefani, M. (2002) Inherent toxicity of aggregates implies a common mechanism for protein misfolding diseases. *Nature* **416**, 507–511
82. Soto, C. (2003) Unfolding the role of protein misfolding in neurodegenerative diseases. *Nat. Rev. Neurosci.* **4**, 49–60
83. Tomokane, N., Iwaki, T., Tateishi, J., Iwaki, A., and Goldman, J. E. (1991) Rosenthal fibers share epitopes with alpha B-crystallin, glial fibrillary acidic protein, and ubiquitin, but not with vimentin: immunoelectron microscopy with colloidal gold. *Am. J. Pathol.* **138**, 875–885
84. Hagemann, T. L., Gaeta, S. A., Smith, M. A., Johnson, D. A., Johnson, J. A., and Messing, A. (2005) Gene expression analysis in mice with elevated glial fibrillary acidic protein and Rosenthal fibers reveals a stress response followed by glial activation and neuronal dysfunction. *Hum. Mol. Genet.* **14**, 2443–2458
85. Norenburg, M. (1997) Astrocytes pathophysiology in disorders of the central nervous system. in *Astrocytes in Brain Aging and Neurodegeneration* (Schipper, H. ed) Landes Bioscience, Austin, TX
86. Price, R. W., and Brew, B. J. (1988) The AIDS dementia complex. *J. Infect. Dis.* **158**, 1079–1083
87. Vitkovic, L., and da Cunha, A. (1995) Role for astrocytosis in HIV-1-associated dementia. *Curr. Top. Microbiol. Immunol.* **202**, 105–116
88. Zou, W., Kim, B. O., Zhou, B. Y., Liu, Y., Messing, A., and He, J. J. (2007) Protection against human immunodeficiency virus type 1 Tat neurotoxicity by Ginkgo biloba extract Egb 761 involving glial fibrillary acidic protein. *Am. J. Pathol.* **171**, 1923–1935
89. Liu, Z., Zhao, F., and He, J. J. (2014) Hepatitis C virus (HCV) interaction with astrocytes: nonproductive infection and induction of IL-18. *J. Neurovirol.* **20**, 278–293
90. Liu, Y., Li, J., Kim, B. O., Pace, B. S., and He, J. J. (2002) HIV-1 Tat protein-mediated transactivation of the HIV-1 long terminal repeat promoter is potentiated by a novel nuclear Tat-interacting protein of 110 kDa, Tip110. *J. Biol. Chem.* **277**, 23854–23863